Journal of Applied Polymer Science

Multifractal Analysis on Dispersion of Immiscible High-Density Polyethylene/Polystyrene Blends Processed via Polymer Vane Plasticating Extruder

Zheng-Huan Wu,[1,2] Yong-Qing Zhao,[1,2] Gui-Zhen Zhang,[1,2] Zhi-Tao Yang,[1,2] Jin-Ping Qu[1,2]

[1]National Engineering Research Center of Novel Equipment for Polymer Processing, South China University of Technology, Guangzhou 510641, China

[2]Key Laboratory of Polymer Processing Engineering of Ministry of Education, South China University of Technology, Guangzhou 510641, China

Correspondence to: Z.-T. Yang (E-mail: meztyang@scut.edu.cn); J.-P. Qu (E-mail: jpqu@scut.edu.cn)

ABSTRACT: A 30 wt % high-density polyethylene (HDPE)/70 wt % polystyrene (PS) blends and 5 wt % HDPE/95 wt % PS blends were prepared via polymer vane plasticating extruder, which can generate elongational force field, in different rotation speeds. The fracture surface of the HDPE/PS blends was observed by a scanning electron microscope, and the dispersion of the HDPE in the PS matrix was evaluated by multifractal programs. The multifractal spectrum width $\Delta\alpha$, and the dimension difference of maximum and minimum probability subset $\Delta f(\alpha)$ were defined to discuss the homogeneity and the diameter of the HDPE particles. The results showed that the multifractal method was an effective tool to quantitatively describe the special distribution and diameter of the dispersed particles. © 2013 Wiley Periodicals, Inc. J. Appl. Polym. Sci. 130: 2328–2335, 2013

KEYWORDS: applications; extrusion; morphology; blends

Received 6 December 2012; accepted 19 April 2013; Published online 22 May 2013
DOI: 10.1002/app.39434

INTRODUCTION

High-density polyethylene and polystyrene are on the list of the most general plastics. HDPE performs well in tenacity, solvent resistance, and low temperature resistance, but has bad rigidity,[1] while PS is just on the contrary.[2] For the purpose of combining their advantages together, i.e., forming better blends and composites, plentiful scientific investigations have been made. According to the thermodynamic criterion, HDPE and PS were thermodynamic immiscible.[3] Whereas, the mechanical compatibility can be improved through varieties of methods.[4] Melt blending is a commonly used method among them.

Referring to the melt blending devices, researchers always use screw extruder, which is mainly dominated by shearing flow field, to process polymer materials. In this experiment, a polymer vane plasticating extruder (PVPE) which developed by Qu is used, the processing principle of which is mainly based on the elongational flow field.[5] Figure 1 indicates the structure of the device. The profile A–A represents the cross section of the PVPE. Nineteen groups of vane plasticating and conveying units (VPCU) constitute the main structure of the PVPE device, which can generate elongational flow field to a certain degree. In VPCU, a space with certain geometric shape is made up by rotors, stators, certain number of vanes and material-proof plates. As the rotor is eccentric to the inter cavity of stators, the volume of which would vary successively according to the order of first ascending then descending. Materials enter into the space while the volume is swelling. Furthermore, materials are grinded, compacted, exhausted by forces of elongation, and compression.[6,7] It can also be seen as a periodical dynamic plasticating conveying procedure.

Dispersion is an important feature of the polymer blends or composites, which has close relationship with polymeric properties, such as compatibility,[8] mechanical properties, and physical properties.[9] Researchers have done many studies on it. It has been demonstrated that the investigation on the microstructure is an effective way to judge the dispersion of the polymer materials.[10,11] However, it is hard to distinguish from the photos when the ratio of the components is the same or even close, while other parameter changes, such as rotation speed, temperature, pressure, and so on. In this case, a quantitative method is needed to determine the quantity of the dispersion.

Fractal theory is used extensively in many scopes after it has been created. Some researchers focus on distinguishing which one has the best homogeneity among several microstructure

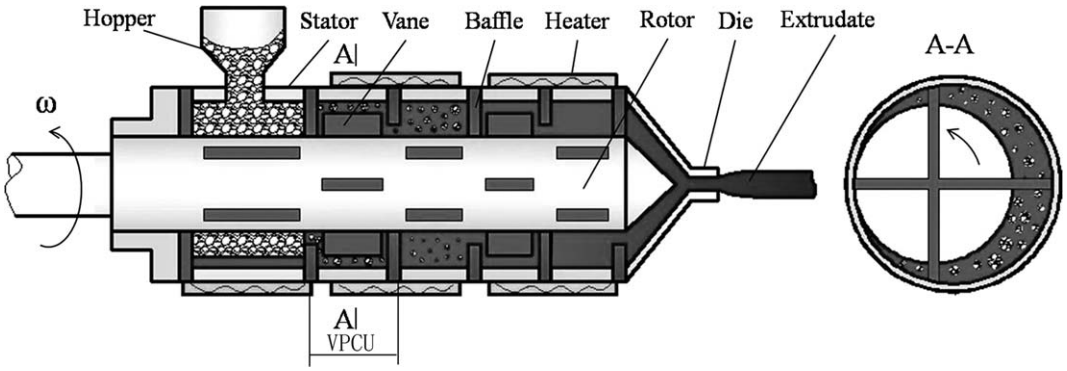

Figure 1. Structure schematic diagram of polymer vane plasticating extruder.[5]

photos by using a fractal method.[12] Other researchers have been investigated the relationship between the dispersion and the mechanical properties of nano-inorganic particles in polymer matrix.[13–15] Actually, a few researchers have paid attention to distinguishing dispersion of immiscible blends.[16,17]

In the research, in order to quantitatively measure the influence that the rotation speed of the PVPE imposed on the dispersion of the same ratio immiscible HDPE/PS blends, matlab programs of multifractal were composed to deal with the SEM images. Related data and figures could be acquired with them. A brief description of the multifractal spectrum program could be explained as follow: The SEM images were imported into the program, implemented with binary treatment, covered by grids with different ε. According to $P_{ij}(\varepsilon)=n_{ij}/\sum n_{ij}$, $\chi_q(\varepsilon)=\sum P_{ij}^q(\varepsilon)$,[18–20] and P_{ij} were calculated, which was used to calculate $\chi_q(\varepsilon)$, According to $\ln\chi_q(\varepsilon)\sim\ln\varepsilon$ curves, the slope $\tau(q)$ was calculated. Based on $\begin{cases}\alpha=d\tau(q)/dq\\ f(\alpha)=\alpha q-\tau(q)\end{cases}$, α, $f(\alpha)$ could be obtained. The curves $f(\alpha)\sim q$, $\alpha\sim q$ were used to indicate the value selection rationality of Δq. The curves $f(\alpha)\sim\alpha$ were the multifractal spectrums.[21] The curves of $\Delta\alpha$, $\Delta f(\alpha)$ with different rotation speeds represented the homogeneity, the particle diameters, separately.

EXPERIMENTAL

Materials

The PS in this study was a granular resin with trade mark of GPPS-525, supplied by Zhanjiang Xinzhongmei Chemical Co., in China. The melt flow index was 8.0 g/10 min (ASTM D-1283). The HDPE used in this study was a granular resin with trade mark of TR144, supplied by Sinopec Maoming Company in China. The melt flow index was 15 g/10 min (ASTM D-1238).

Samples Preparation

The experiments were divided into two groups. In the first group, without any treatment, 30 wt % HDPE resin and 70 wt % PS resin were mixed and extruded via the polymer vane plasticating extruder in different rotation speeds, which were separately 30, 45, 60, 75, and 90 r/min. The processing temperatures of four sections in the polymer vane plasticating extruder were separately 170, 220, 220, and 210°C. In the second group, other parameters were still the same except the ratio of the HDPE/PS blends changed into 5 wt %/95 wt %.

Morphological Test

Scanning electron microscopy (SEM) tests revealed the fracture surfaces of the HDPE/PS blends, which were taken by a Hitachi Scanning Electronic Microscope (SEM, model S-3700N, Japan), the samples were submerged in liquid nitrogen for about 10 min, and fractured to expose the internal structure for SEM investigations. Prior to the morphological test, all surfaces were sputtered with gold twice to provide enhanced conductivity.

RESULTS AND DISCUSSION

Fracture Morphology

Figures 2 and 3 are the SEM images of the fracture surface morphology, of which "A" represents group of 30 wt % HDPE/70 wt % PS blends, "B" represents group of 5 wt % HDPE/95 wt % PS blends; "1," "2," "3," "4," and "5" represent rotation speeds of 30, 45, 60, 75, and 90 r/min, respectively. The HDPE/PS blends were mixed well, which made it hard to define which one had the best dispersion. Multifractal program was carried out to select the figure with the best dispersion.

Multifractal Analysis Based on SEM Fracture Morphology

Figures 4 and 5 are the $\ln\varepsilon\sim\ln\chi_q(\varepsilon)$ curves of 30 wt % HDPE/70 wt % PS blends and 5 wt % HDPE/95 wt % PS blends at different rotation speeds, respectively. It could be counted from each figure that there were 25 lines from top to bottom. It indicated that different values of q had different curves of $\ln\varepsilon\sim\ln\chi_q(\varepsilon)$ to correspond. The curves were marked with different value of q in A_1 and B_1. A_2–A_5 and B_2–B_5 were the same. All the curves could be divided into linear section and nonlinear section. Every nonlinear section fluctuated in different degree. Take A_1 of Figure 4 for example.

The $\ln\varepsilon\sim\ln\chi_q(\varepsilon)$ curves varied linearly when q was in [0, 6], which changed nonlinearly when q was in [−6, 0], especially when $\ln\varepsilon$ was in [−4.852, −2.773]. The linear section indicated that $\ln\chi_q(\varepsilon)$ had fine scale invariance in all ε ranges.[22] The existing of the nonlinear section revealed that it would not suitable for the requirement of the scale invariance in all ε ranges, the larger absolute value of the slope lead to bigger ε, and vice versa. The odd phenomenon had close relationship with the

Applied Polymer SCIENCE

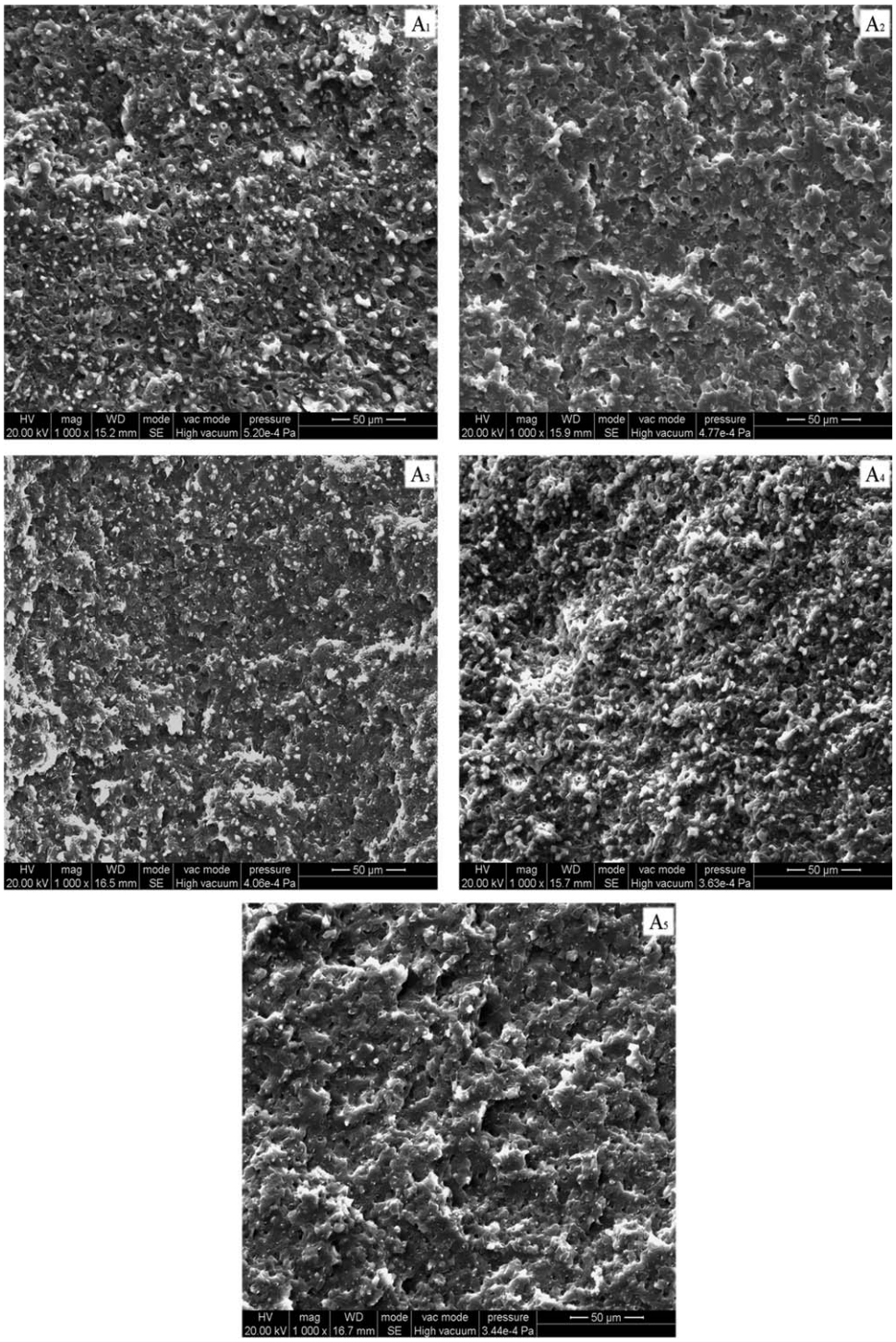

Figure 2. Morphology of 30 wt % HDPE/70 wt % PS blends at different rotation speeds.

exceptional swing of the small probability. As graphic fragments with a few pixels would occur in box-counting processing, therefore, $P(\varepsilon)$ might decrease excessively with the reduction of the ε, which lead to χ_q increase exceptionally. As ε continue to decline, $P(\varepsilon)$ with one pixel would grow in number, for the pixel would not be subdivided infinitely. In the equation $P_{ij}(\varepsilon)=n_{ij}/\sum n_{ij}$, when $P_{ij}(\varepsilon)$ became the smallest, the numerator n_{ij} would be 1, and the total pixels $\sum n_{ij}$ in the denominator would be a constant value, which made the value of the smallest $P_{ij}(\varepsilon)$ would not decline with the decreasing of the ε. Afterwards, the corresponding $\chi_q(q \in (-6,1))$ would decline rather slowly (the number of the smallest $P_{ij}(\varepsilon)$ would increase with the reducing of the ε, but would have little effect in χ_q), which caused the $\chi_q(q \in (-6,0))$ value less than normal.[23,24]

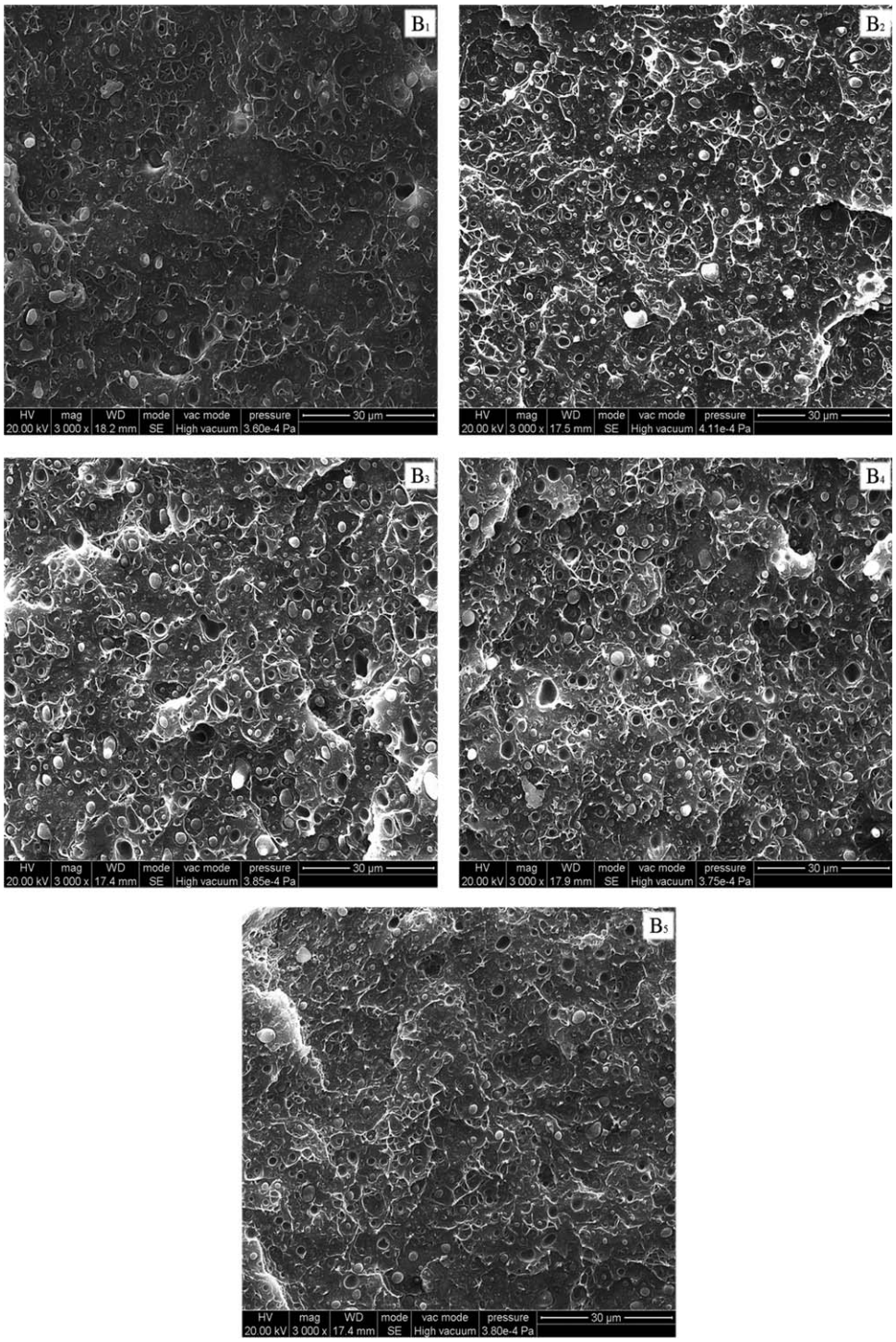

Figure 3. Morphology of 5 wt % HDPE/95 wt % PS blends at different rotation speeds.

In the multifractal program, q was set in the range of $[-6, 6]$, and the absolute value of Δq was set as 0.5. In Figure 6, α varied fiercely when q was in the range of $[-4, 1]$, and fluctuated small when q was in the range of $[-6, -4]$ and $[1, 6]$. It could be observed from Figure 7 that $f(\alpha)$ varied fiercely when q was in the range of $[-4, 0]$, and fluctuated small when q was in the range of $[-6, -4]$ and $[0, 6]$. It meant that the value selection of q and Δq was reasonable. Namely the multifractal spectrum $f(\alpha)$ achieved the probability distribution requirement. The absolute value of q should be set larger than 6 if α and $f(\alpha)$ still varied fiercely at the end of the q range.

In Figure 8, $f_{\max}(\alpha)$ in different rotation speeds had minimal difference, all concentrated at $\alpha=2$, and around, which

Applied Polymer SCIENCE

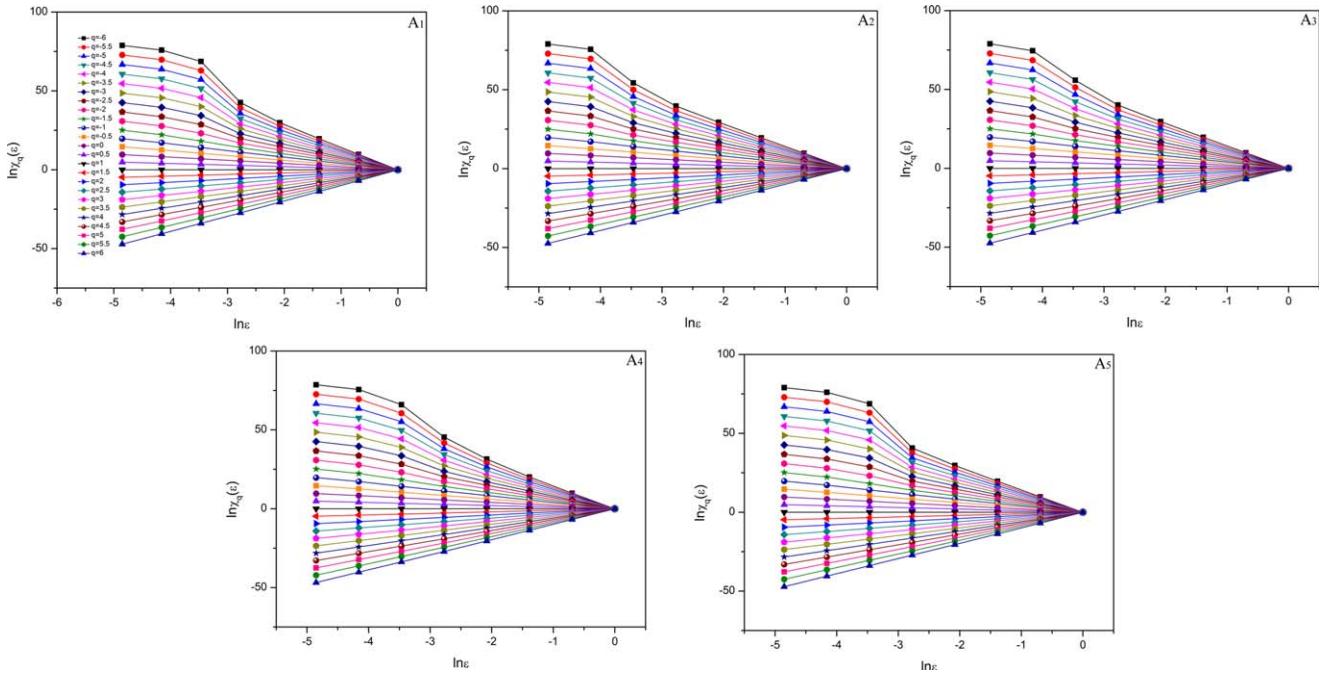

Figure 4. ln ε ~ln $\chi_q(\varepsilon)$ curves of 30 wt % HDPE/70 wt % PS blends at different rotation speeds. [Color figure can be viewed in the online issue, which is available at wileyonlinelibrary.com.]

indicated that the dispersed phase particles occupied the similar region in each group.[23,24] As the ratio of A(B) series was identical, The area of the HDPE in the PS zone would not change significantly with the variation of the rotation speed.

From Figure 8, because the scale of the box was less than $1(\varepsilon \leq 1)$, the value of the largest probability of the distribution $P_{ij}(\varepsilon) \sim \varepsilon^{\alpha_{min}}$ would be larger if α_{min} were smaller. And the larger value of α_{max} made the smallest distribution probability $P_{ij}(\varepsilon) \sim \varepsilon^{\alpha_{max}}$ value smaller.[25] The homogeneity of the probability distribution could be expressed by multifractal spectrum width $\Delta\alpha$:

$$\Delta\alpha = \alpha_{max} - \alpha_{min} = \ln(P_{max}/P_{min})/ln(1/\varepsilon)$$

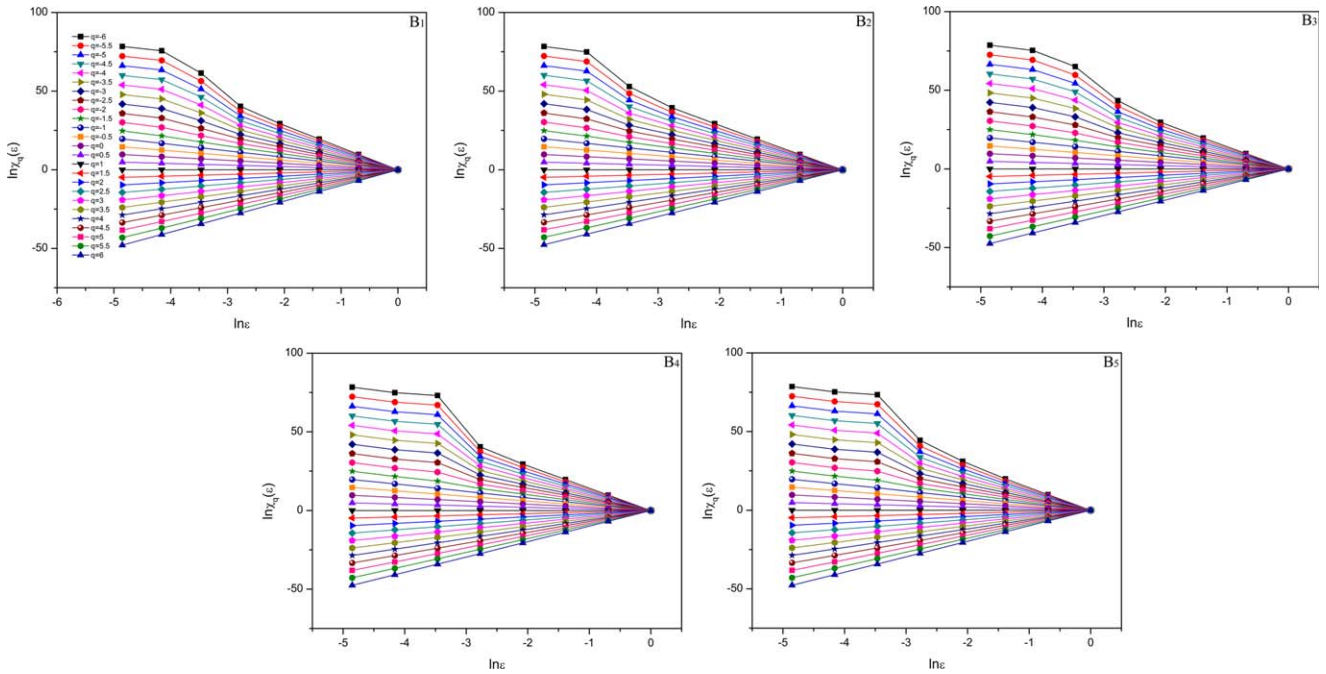

Figure 5. ln ε ~ln $\chi_q(\varepsilon)$ curves of 5 wt % HDPE/95 wt % PS blends at different rotation speeds. [Color figure can be viewed in the online issue, which is available at wileyonlinelibrary.com.]

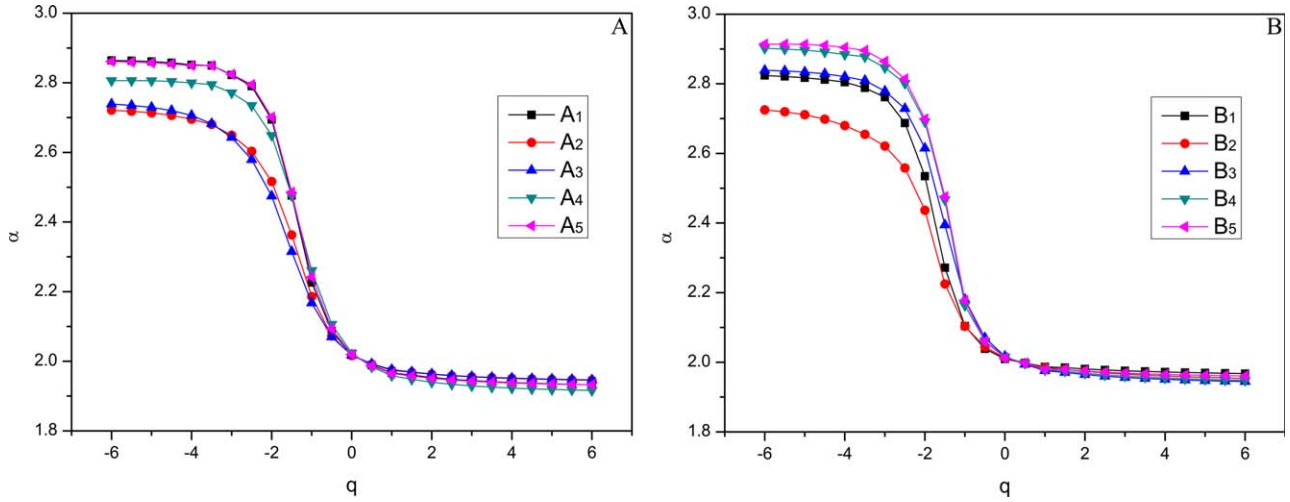

Figure 6. q ~ α curves at different rotation speeds. [Color figure can be viewed in the online issue, which is available at wileyonlinelibrary.com.]

The equation above demonstrated that the smaller $\Delta\alpha$ value indicated the better homogeneity. Under the ideal condition, it was the most homogeneous when $\Delta\alpha=0$.[26] Combining with Table I, the dispersion homogeneity could be arranged from the best to the worst: A_2, A_3, A_4, A_1, A_5; And B_2, B_1, B_3, B_5, B_4. Though the orders of two groups were different, Figure 9 and Table I reflected the same tendency. Both A and B groups had the best homogeneity when the rotation speed was 45 r/min, and the homogeneity was better when the rotation speed was in the range of 30–60 r/min. Furthermore, the homogeneity of both A and B groups were worse when the rotation speed was over 60 r/min.

$$\Delta f(\alpha)=f(\alpha_{\min})-f(\alpha_{\max})=\ln\left(N_{P_{\min}}/N_{P_{\max}}\right)/\ln\varepsilon$$

The equation above represented the dimension difference between maximum probability subset and minimum probability subset, $f(\alpha_{\min})$ and $f(\alpha_{\max})$ represented the maximum probability and the minimum probability. In the research, the positive and negative of the $\Delta f(\alpha)$ value could be understood as the ratio between the large diameter particle number and the small diameter particle number. The number of the large diameter particle was more than that of the small diameter particle when $\Delta f(\alpha) > 0$, and vice versa.[23,24] Figure 10 shows that the $\Delta f(\alpha)$ values of both two groups of blends are positive with the growth of the rotation speed, which suggests that the number of the large diameter particles is more than that of the small diameter particles in the fracture surface.

Besides, for the two groups of blends, with the growth of the rotation speed, the number of the large diameter particles both decreased and then increased, both the minimum numbers occurred at the rotation speed of 60 r/min. Due to the premise of the multifractal statistics in the research was the scale invariance, which meant that both two groups of blends possessed the minimum size of dispersed particles when the rotation speed was 60 r/min.

The symmetry of $\alpha \sim f(\alpha)$ curves was also considered as one of the important characteristics. Multifractal spectrums are hook-like or bell-like curves.[27] Figure 8 showed that all $\alpha \sim f(\alpha)$ curves presented as left hook, though in different curve degree.

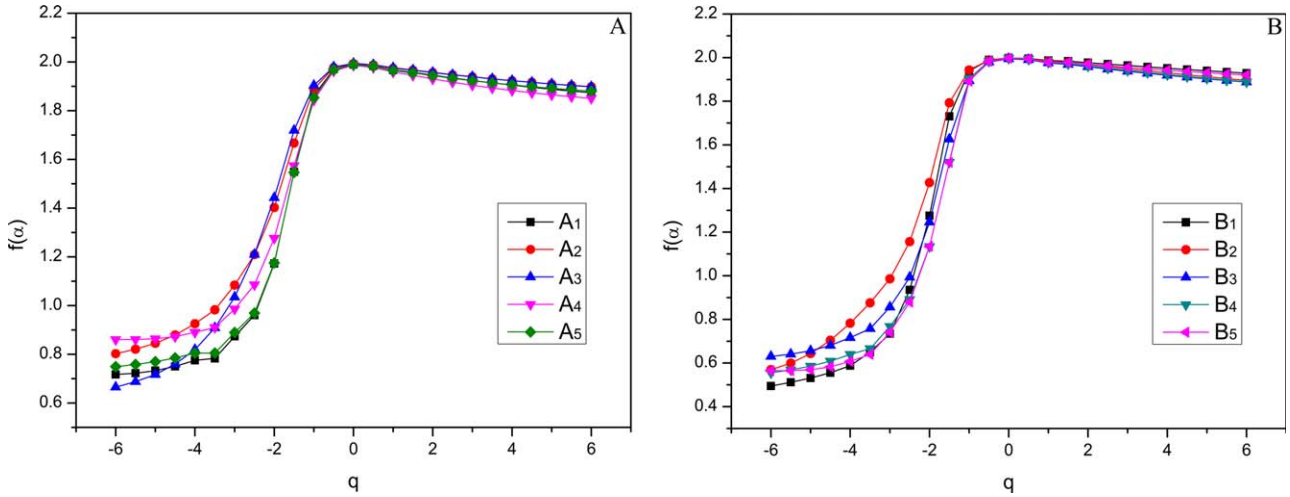

Figure 7. q ~ f curves at different rotation speeds. [Color figure can be viewed in the online issue, which is available at wileyonlinelibrary.com.]

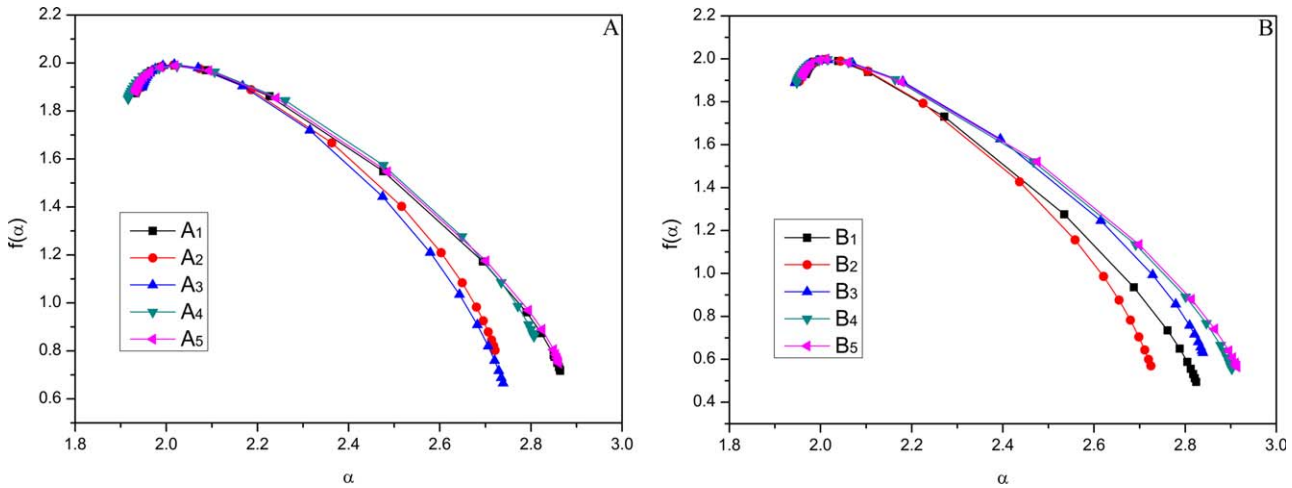

Figure 8. $\alpha \sim f(\alpha)$ curves at different rotation speeds. [Color figure can be viewed in the online issue, which is available at wileyonlinelibrary.com.]

It revealed that the number of the big probability subsets was larger than that of the small probability subsets. There were two possible explanations. The number of the high density particle aggregation zone was more than that of low density particles aggregation zone; the number of large size particles was larger than that of small size particles in dispersed phase.[28,29] According to Figures 2 and 3, the last explanation would be more reasonable.

Zhang et al.[7] set pressure sensor in the PVPE, and recorded the pressures at different rotation speeds. The result showed that the pressure that imposed on the LDPE increased during mixing processing with the rotation speed increasing, which indicated that the elongational force field component that generated by the PVPE had relationship with the inherent structural parameters and the intrinsic characteristics of the materials, and also connected with the processing parameters. It seemed that the higher rotation speed caused the better mixing effect. In other words, the dispersion would be better with the higher rotation speed. However, the experimental result of the multifractal analysis was not in accordance with the theoretical value.

Yang, et al.[6] reported the relationship between the unit yield of the LDPE and the rotation speed, an approximate linear relation was obtained between them. It implied that the residence time of the materials in the PVPE became less with the higher rotation speed. The less mixing time that imposed on the materials would cause the worse dispersion of the blends.

As the elongational force field and the residence time existed simultaneously, it could be speculated that in order to obtain the best dispersion, an optimal rotation speed range should be existed when other processing parameters were fixed, which made the elongational force field strength large enough, and the material residence time long enough. The optimal speed range was 45–60 r/min in the discussion. Furthermore, for both two ratios of HDPE/PS blends, the same optimal rotation speed range and the similar dispersion tendency could be obtained from the multifractal program, which made the result reliable to a certain degree.

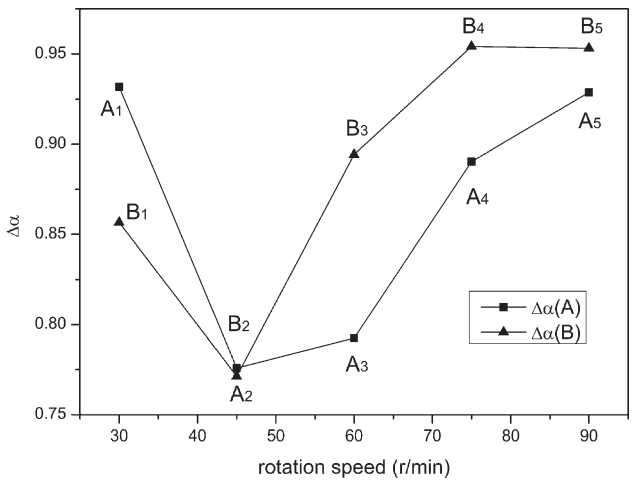

Figure 9. $\Delta\alpha$ curves at different rotation speeds.

CONCLUSION

The dispersion of 30 wt % HDPE/70 wt % PS and 5 wt % HDPE/95 wt % PS blends had been quantitatively estimated by multifractal method. The results indicated that both two ratios of HDPE/PS blends had the same variation tendency of the homogeneity and the diameter. With the rotation speed increasing, the homogeneity increased first and then decreased, the

Table I. Multifractal Spectrum Width $\Delta\alpha$ with Different Rotation Speeds

Rotation Speed (r/min)	30	45	60	75	90
$\Delta\alpha$(A)	A_1	A_2	A_3	A_4	A_5
	0.9318	0.7759	0.7925	0.8903	0.9288
$\Delta\alpha$(B)	B_1	B_2	B_3	B_4	B_5
	0.8567	0.7713	0.8943	0.9542	0.9532

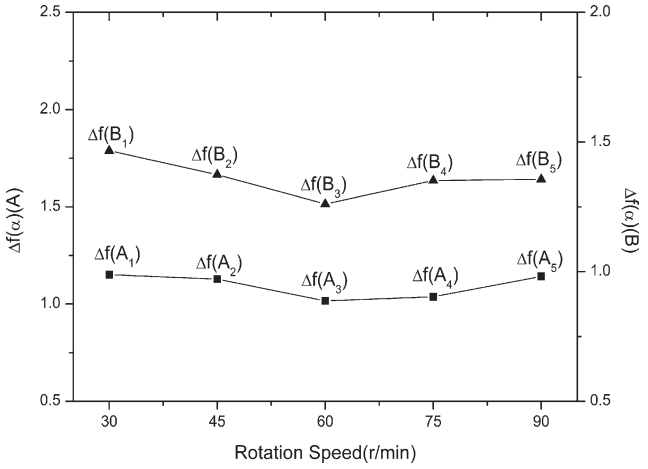

Figure 10. $\Delta f(\alpha)$curves at different rotation speeds.

dispersed phase diameter decreased first and then increased, and the best dispersion both occurred in the rotation speed range of 45–60 r/min. this conclusion implied us that if a fine dispersion of immiscible blends that proceed via the polymer vane plasticating extruder were needed, the rotation speed which around 45–60 r/min should be considered preferentially.

NOMENCLATURE

ε	Measurement scale.
P_{ij}	Distributions of probability measurement of pixels.
$P_{ij}(\varepsilon) \sim \varepsilon^{\alpha_{\min}}$	The largest probability of distribution.
n_{ij}	Amount of pixels in each box.
$\sum n_{ij}$	Total amount of pixels boxes.
q	Weight factor.
q_{init}	Initial value.
Δq	Step length.
$\chi_q(\varepsilon)$	Distribution functions.
$\ln \chi_q \sim \ln \varepsilon$	Slopes of the double logarithmic coordinates.
α	Singularity index.
$\Delta\alpha$	Spectrum width.
$\tau(q)$	Weight index.
$f(\alpha)$	Multifractal spectrum.
$f_{\max}(\alpha)$	Maximum value of multifractal spectrum.
$f(\alpha_{\min})$	Dimension of maximum probability subset.
$f(\alpha_{\max})$	Dimension of minimum probability subset.
$\Delta f(\alpha)$	Dimension difference between maximum and minimum probability subset.
$N_{P_{\min}}$	Particle number of minimum probability subset.
$N_{P_{\max}}$	Particle number of maximum probability subset.

ACKNOWLEDGMENTS

The authors wish to acknowledge the National Nature Science Foundation of China (Grant 10872071, 50973035 and 50903033), the Fundamental Research Funds for the Central Universities (NO.2011ZM0063) and National Key Technology R&D Program of China (Grant 2009BAI84B05 and 2009BAI84B06) for the financial supports, Program for New Century Excellent Talents in University(No.NCET-11-0152) and Pearl River Talent Fund for Young Sci-Tech Researchers of Guangzhou City (No.2011J2200058) for financial support.

REFERENCES

1. Tjong, S. C.; Xu, S. A. *J. Appl. Polym. Sci.* **1998**, *68*, 1099.
2. Wu, J. S.; Guo, B. H.; Chan, C. M.; Li, J. X.; Tang, H. S. *Polymer* **2001**, *42*, 8858.
3. Barlow, J. W.; Paul, D. R. *Polym. Eng. Sci.* **1984**, *24*, 525.
4. Nandan, B.; Lal, B.; Pandey, K. N. *Eur. Polym. J.* **2001**, *24*, 2148.
5. Qu, J. P. Can. Pat. CN200810026054X, June 10, **2009**.
6. Qu, J. P.; Yang, Z. T.; Yin, X. C.; He, H. Z.; Feng, Y. H. *Polym. Plast. Technol. Eng.* **2009**, *48*, 1269.
7. Qu, J. P.; Zhang, G. Z.; Chen, H. Z.; Yin, X. C.; He, H. Z. *Polym. Eng. Sci.* **2012**, *52*, 2148.
8. Mitchell, C. A.; Bahr, J. L.; Arepalli, S.; Tour, J.M; Krishnamoorti, R. *Macromolecules* **2002**, *35*, 8825.
9. Chen, C. C.; White, J. L. *Polym. Eng. Sci.* **1993**, *33*, 923.
10. Singh, R. P.; Zhang, M.; Chan, D. *J. Mater. Sci.* **2002**, *37*, 785.
11. Hussain, M.; Oku, Y.; Nakahira, A.; Niihara, K. *Mater. Lett.* **1996**, *29*, 180.
12. Halsey, T. C.; Jensen, M. H.; Kadanoff, L. P.; Procaccia, I.; Shraiman, B. I. *Phys. Rev. A* **1986**, *33*, 1141.
13. Mandelbrot, B. B.; Passoja, D. E.; Paulla, A. J. *Nature* **1984**, *19*, 721.
14. Zhen, J.; Ding, Y. F.; Du. J. Q. *Plast. Proc. Appl.* **2001**, *23*, 5.
15. Liang, J. Z. *Compos. Part A Appl. S* **2007**, *38*, 1506.
16. Yan, L. T.; Sheng, J. *Polymer* **2006**, *47*, 2894.
17. Patlazhan, S.; Schlatter, G.; Serra, C.; Bouquey, M.; Muller, R. *Polymer* **2006**, *47*, 6099.
18. Halsey, T. C.; Duplantier, B.; Honda, K. *Phys. Rev. Lett.* **1997**, *78*, 1719.
19. Balankin, A. S.; Izotov, A. D.; Novikov, V. U. *Inorg. Mater.* **1999**, *35*, 1047.
20. Feng, Y. F.; Shang, J. Y. *Electric. Power Sci. Eng.* **2011**, *27*, 61.
21. Stanley, H. E.; Meakin, P. *Nature* **1988**, *335*, 407.
22. Schertzer, D.; Joy, S. L. *Int. J. Bifurcat. Chaos.* **2011**, *21*, 3418.
23. Pérez, E.; Bernal, C.; Piacquadio, M. *Appl. Surf. Sci.* **2012**, *258*, 8941.
24. Zhang, Y. H.; Bai, B. F.; Li, J. Q.; Chen, J. B.; Shen, C. Y. *Appl. Surf. Sci.* **2011**, *257*, 2985.
25. Zhang, Y. H.; Bai, B. F.; Chen, J. B.; Shen, C. Y.; Li, J. Q. *Appl. Surf. Sci.* **2010**, *256*, 7152.
26. Li, H.; Ding, Z. J.; Wu, Z. Q. *Phys. Rev.* **1995**, *51*, 13558.
27. Li, H.; Ding, Z. J.; Wu, Z. Q. *Phys. Rev.* **1996**, *53*, 16634.
28. Wang, M.; Liu, X. Y.; Strom, C. S.; Bennema, P.; Enckevort, W. V.; Ming, N. B. *Phys. Rev. Lett.* **1998**, *80*, 3092.
29. Liu, C.; Jiang, X. L.; Liu, T.; Zhao, L.; Zhou, W. X.; Yuan, W. K. *Appl. Surf. Sci.* **2009**, *255*, 4240.